Is the Mammalian Cell Plasma Membrane a Barrier to Oxygen Transport?

WITOLD K. SUBCZYNSKI, LARRY E. HOPWOOD, and JAMES S. HYDE

From the National Biomedical Electron Spin Resonance Center, Department of Radiology and Department of Radiation Oncology, Medical College of Wisconsin, Milwaukee, Wisconsin 53226; and Department of Biophysics, Institute of Molecular Biology, Jagiellonian University, 31-120 Krakow, Poland

ABSTRACT Oxygen transport in the Chinese hamster ovary (CHO) plasma membrane has been studied by observing the collision of molecular oxygen with nitroxide radical spin labels placed in the lipid bilayer portion of the membrane at various distances from the membrane surface using the long-pulse saturation–recovery electron spin resonance (ESR) technique. The collision rate was estimated for 5-, 12-, and 16-doxylstearic acids from spin-lattice relaxation times (T_1) measured in the presence and absence of molecular oxygen. Profiles of the local oxygen transport parameters across the membrane were obtained showing that the oxygen diffusion–concentration product is lower than in water for all locations at 37°C. From oxygen transport parameter profiles, the membrane oxygen permeability coefficients were estimated according to the procedure developed earlier by Subczynski et al. (Subczynski, W. K., J. S. Hyde, and A. Kusumi. 1989. *Proceedings of the National Academy of Sciences, USA.* 86:4474–4478). At 37°C, the oxygen permeability coefficient for the plasma membrane was found to be 42 cm/s, about two times lower than for a water layer of the same thickness as the membrane. The oxygen concentration difference across the CHO plasma membrane at physiological conditions is in the nanomolar range. It is concluded that oxygen permeation across the cell plasma membrane cannot be a rate-limiting step for cellular respiration. Correlations of the form $P_M = cK^s$ between membrane permeabilities P_M of small nonelectrolyte solutes of mol wt <50, including oxygen, and their partition coefficients K into hexadecane and olive oil are reported. Hexadecane: $c = 26$ cm/s, $s = 0.95$; olive oil: $c = 23$ cm/s, $s = 1.56$. These values of c and s differ from those reported in the literature for solutes of $50 <$ mol wt <300 (Walter, A., and J. Gutknecht. 1986. *Journal of Membrane Biology.* 90:207–217). It is concluded that oxygen permeability through membranes can be reliably predicted from measurement of partition coefficients.

INTRODUCTION

Knowledge of the concentration, diffusion, and transport of molecular oxygen in tissues, cells, and subcellular structures is required to solve important oxygen-related

Address reprint requests to Dr. Witold K. Subczynski, National Biomedical ESR Center, 8701 Watertown Plank Road, Milwaukee, WI 53226.

J. GEN. PHYSIOL. © The Rockefeller University Press · 0022-1295/92/07/0069/19 $2.00
Volume 100 July 1992 69–87

physiological and toxicological problems (McCord, 1985) and to understand the basis for radiation (Hill and Pallavicini, 1983) and photodynamic (Kalyanaraman, Feix, Sieber, Thomas, and Girotti, 1987) therapy.

The rate of oxygen consumption of a suspension of cells can be measured using various approaches (Lai, Hopwood, Hyde, and Lukiewicz, 1982; Froncisz, Lai, and Hyde, 1985, and citations therein). It was found in these two studies that the rate of oxygen consumption of Chinese hamster ovary (CHO) cells was independent of dissolved oxygen concentration down to levels as low as ~1 μM. It is therefore apparent that the respiratory rate in this cellular system is under enzymatic control over a wide range of oxygen tensions, and the question of whether or not the membrane is a barrier to oxygen transport can be relevant only at low concentrations. Froncisz et al. (1985) developed arguments indicating that diffusion limitation in the CHO system cannot be occurring at any level of oxygen concentration including concentrations near the apparent Michaelis-Menten value. However, this conclusion was cautiously qualified. The question of whether or not diffusion limitation can occur either from diffusion limitation in the surrounding medium or in the cell membrane is a fundamental one of considerable importance. The present study approaches this question in another way by asking how the barrier to oxygen transport presented by the membrane compares with that of the surrounding medium.

Because oxygen is constantly consumed, and oxygen consumption reactions are localized inside the cell, it follows that there must be a gradient in oxygen concentration across the cell plasma membrane. The value of the oxygen concentration difference is determined by the rate of oxygen consumption by the cell and the oxygen permeability coefficient of the cell plasma membrane. Values of oxygen concentration differences reported in the literature vary widely: from small, lower than 1 μM (Katz, Wittenberg, and Wittenberg, 1984; Wittenberg and Wittenberg, 1985), to large, a few micromolar to as great as 40 μM (Tamura, Oshino, Chance, and Silver, 1978; Jones and Kennedy, 1982; Jones, 1984; Morse and Swartz, 1985; Glockner, Swartz, and Pals, 1989; see also review papers by Swartz and Pals, 1988; and Wittenberg and Wittenberg, 1989).

Direct measurement of the oxygen concentration difference across a cell plasma membrane of oxygen-consuming cells is difficult because it must be done using oxygen-sensitive probes both outside and inside the cell (Swartz and Pals, 1988). Another approach is to calculate the concentration difference on the basis of a measured oxygen consumption rate and the plasma membrane permeability coefficient for oxygen.

Attempts have been made to determine the oxygen membrane permeability coefficient using stop-flow rapid-mixing apparatus to create an oxygen gradient. These studies have been criticized because the presence of a thick (~2 μm) unmixed water layer on the cell surface prevents immediate contact of the oxygenated solution with the cell membrane (Coin and Olson, 1979; Huxley and Kutchai, 1981, 1983). Other studies have been reported using the quenching of fluorescence or phosphorescence probes by oxygen in red blood cell membranes, mitochondrial membranes, or artificial membranes to obtain insight into oxygen permeability. However, these methods give only the average oxygen diffusion–concentration product across the membrane because of the large size of the probe and its uncertain localization in the membrane (Fischkoff and Vanderkooi, 1975; Vanderkooi, Wright, and Erecinska,

1990). Nuclear magnetic resonance techniques give a good spatial distribution of the oxygen diffusion–concentration product across the membrane, but the sensitivity of the method is low (McDonald, Vanderkooi, and Oberholtzer, 1979).

In our previous papers we developed a methodology to estimate the membrane oxygen permeability coefficient from the profile of the oxygen diffusion–concentration product across the membrane (Subczynski, Hyde, and Kusumi, 1989, 1991*a*; Subczynski and Markowska, 1992). Our method is based on a theory by Diamond and Katz (1974) and does not need creation of fast decaying oxygen gradients. Profiles of the oxygen diffusion–concentration product across the membrane can be obtained using different electron spin resonance (ESR) spin-label approaches: line-broadening (Windrem and Plachy, 1980; Subczynski and Markowska, 1992), continuous wave saturation (Subczynski and Hyde, 1981), or saturation recovery (Kusumi, Subczynski, and Hyde, 1982; Subczynski et al., 1989, 1991*a*). The present study uses the long-pulse saturation–recovery ESR technique to investigate oxygen transport in the plasma membrane of CHO cells by observing the collision of molecular oxygen with nitroxide radical spin labels placed at various distances from the membrane surface. The value of the membrane oxygen permeability coefficient is determined from the profile of the oxygen diffusion–concentration product across the cell plasma membrane, and the oxygen concentration difference under physiological conditions is then calculated. A description of the mathematical procedure is also given.

It is commonly accepted that stearic acid spin labels reside in the lipid bilayer portion of the cell membrane (Kaplan, Canonico, and Caspary, 1973; Bales, Lesin, and Oppenheimer, 1977). However, the exact location of the spin labels within the cell has long been a subject of discussion. Recently, Nettleton, Morse, Dobrucki, Swartz, and Dodd (1988), based on concentration-dependent broadening of the ESR spectra of the nitroxide 5-doxylstearic acid, concluded that the spin label must distribute into most cellular membranes of intact cells. There is also a body of evidence that supports the hypothesis that either a substantial portion of the label resides in the plasma membrane or the ESR signal arises mainly from the cell surface–located spin labels (Kaplan et al., 1973; Gaffney, 1975; Bales et al., 1977; Struve, Arneson, Chenevey, and Cartwright, 1977; Bales and Leon, 1978; Lai, Hopwood, and Swartz, 1980*a*; Dodd, Schor, and Rushton, 1982). Support for the plasma membrane location of stearic acid spin labels comes from the facts that: (*a*) spin labels are rapidly reduced at physiological conditions when entering the cell interior, (*b*) $K_3Fe(CN)_6$, which is impermeable to cell membranes, can quickly reoxidize nitroxides that are reduced by the cell, resulting in revived ESR signals that are identical to the original signals, and (*c*) order parameters measured within minutes after label introduction are the same as those measured later. In this paper we assume the plasma membrane location of stearic acid spin labels, but we will return to that subject in the conclusion.

MATERIALS AND METHODS

Chemicals

5-, 12-, and 16-doxylstearic acid spin labels (5-, 12-, and 16-SASL) were obtained from Molecular Probes, Inc. (Eugene, OR) and 1-^{15}N-1-oxylo-4-oxo-2,2,6,6,-tetramethylpiperidine-

d_{16} (d-TEMPONE) was purchased from Merck Sharp and Dohme/Isotopes (Dorval, Québec, Canada).

Spin Labeling of CHO Cells

Labeling of CHO cells with fatty acid spin labels was carried out as described previously (Lai, Hopwood, and Swartz, 1980*b*). Briefly, 3×10^6 cells from an asynchronous population grown in spinner culture were centrifuged at 4°C at 300 *g* for 5 min and washed once with cold phosphate-buffered saline. A spin-label solution was prepared by drying an ethanolic solution of stearic acid spin label (SASL) under N_2 in a 10-ml beaker, adding 2 ml of phosphate-buffered saline, and stirring vigorously for 5 min at 23°C. 2 ml of cell suspension was gently transferred to the spin-label solution and incubated at 23°C for 10 min with slow stirring (1 rev/s). The concentration of spin labels used in this study was in the range of 12–30 μM. The spin-labeling procedure did not affect cell viability as indicated by plating efficiency (70–80%) or by the mitotic index determined using the hypotonic squash method. The spin-labeled CHO cells were washed twice. The last rinse contained 5 mM KCN to inhibit cell respiration. The thick cell suspension was transferred to a thin wall, 0.6-mm-i.d., gas-permeable capillary made from the methylpentene polymer, TPX (Hyde and Subczynski, 1989). This plastic is permeable to oxygen, nitrogen, and other gases and is substantially impermeable to water. The active sample volume was ~2 μl.

Saturation–Recovery ESR Measurements

The sample in a TPX capillary was positioned inside the loop-gap resonator (Froncisz and Hyde, 1982) of the X-band saturation–recovery spectrometer. The spectrometer is based on the design of Huisjen and Hyde (1974). Control of the concentration of oxygen in the sample was achieved by equilibrating it with the same gas that was used for temperature control, i.e., a mixture of nitrogen and air adjusted with flowmeters (model 7631H-604, Matheson Gas Products, Secaucus, NJ). Spin-lattice relaxation times (T_1's) of spin labels were measured using the long-pulse saturation–recovery technique (Kusumi et al., 1982; Subczynski et al., 1989, 1991*a*). With long and intense pulses, the spin system approaches a steady state in which the populations of all energy levels tend to be equalized. After the saturating pulse is turned off, the recovery of the spin system to Boltzmann equilibrium is observed with a weak observing power. Typically, $1.25–2.5 \times 10^4$ decays per second were accumulated with 256 data points on each decay. Total accumulation time was typically 10 or 20 min. All measurements of T_1 were made on the central line of the ESR spectrum for 5-, 12-, and 16-SASL, and d-TEMPONE at 10, 20, and 37°C. The values of T_1 were obtained by fitting the tails of the saturation–recovery signals to a single exponential.

Processing of Data

The rationale of the spin-label T_1 method is that the molecular probe can be placed at a known location in the membrane to observe local events and that the time scale of T_1 (1–20 μs) is in the correct range to study many molecular processes (Yin and Hyde, 1987). One of these processes is oxygen transport within the membrane. Bimolecular collisions of molecular oxygen (a fast relaxing paramagnetic species) and the nitroxide (a slow relaxing paramagnetic species) induce spin exchange, which leads to faster effective spin-lattice relaxation of the nitroxide. The bimolecular collision rate was evaluated by measuring the T_1's of the nitroxide as a function of the partial pressure of oxygen. An oxygen transport parameter $W(x)$ was introduced as a convenient quantitative measure of the collision rate between the spin label and molecular oxygen (Kusumi et al., 1982).

$$W(x) = T_1^{-1}(\text{air}, x) - T_1^{-1}(N_2, x) \tag{1}$$

Note that $W(x)$ is normalized to the sample equilibrated with atmospheric air. $W(x)$ is proportional to the local concentration $C(x)$ and the local translational diffusion coefficient $D(x)$ of oxygen at a "depth" x in the membrane (which is in equilibrium with atmospheric air):

$$W(x) = AD(x)C(x) \tag{2}$$

where $A = 8\pi p r_0$. Here r_0 is the interaction distance between oxygen and the nitroxide radical spin label ($\sim$4.5 Å) and p is the probability that an observable event occurs when a collision occurs (Hyde and Subczynski, 1984; Subczynski and Hyde, 1984). Membrane profiles of $W(x)$ were constructed on the basis of measurements with SASL spin labels.

Permeability of the membrane to oxygen (P_M) can be calculated from a $W(x)$ profile on the basis of a theory by Diamond and Katz (1974), according to the procedure developed by Subczynski et al. (1989). It is assumed that oxygen diffusion is isotropic.[1] Values of P_M were determined from $W(x)$ by integration:

$$P_M = \frac{1}{AC_W(\text{air})}\left[\int_0^{\delta_M} \frac{dx}{W(x)}\right]^{-1} \tag{3}$$

Possible error arises from the uncertainty of $A(=8\pi p r_0)$ in Eq. 2. Since A is remarkably independent of solvent viscosity, temperature, hydrophobicity, and spin-label species (Hyde and Subczynski, 1984, 1989; Subczynski and Hyde, 1984), the ratio of the permeability coefficient across the membrane (P_M) to the permeability across a water layer of the same thickness as the membrane (P_W) obtained from W_0 (d-TEMPONE) can be evaluated using Eq. 4.[2]

$$P_W = \frac{1}{AC_W(\text{air})}\frac{W_0(\text{d-TEMPONE})}{\delta_M} \tag{4}$$

In Eqs. 3 and 4, δ_M is the entire thickness of the lipid bilayer and C_W(air) is the oxygen concentration in water equilibrated with air at a given temperature. The permeability coefficient of oxygen in a water layer of thickness δ_M can be determined from the macroscopic diffusion coefficient in bulk water (D_W) (St. Denis and Fell, 1971) according to the equation:

$$P_W = D_W/\delta_M \tag{5}$$

Using T_1 measurements in membrane and in water, we determined the ratio P_M/P_W, and using the value of P_W obtained in Eq. 5, we arrived at a value for the oxygen permeability coefficient across the membrane.

[1] We have previously shown that oxygen diffusion is almost isotropic in the liquid-crystalline phase of non–cholesterol-containing membranes (Kusumi et al., 1982). Diffusion of oxygen below the pretransition temperature was found to be more rapid in the transverse than in the lateral direction.

[2] In principle, according to the Smoluchowski equation, $W(x)$ is proportional to the sum of the diffusion coefficient of oxygen and that of the nitroxide spin label. In the membrane, the diffusion coefficient of the stearic acid spin labels can be ignored relative to oxygen. However, for collisions of d-TEMPONE with oxygen in the aqueous phase, it cannot be neglected and W(d-TEMPONE) is a lumped transport parameter for oxygen and d-TEMPONE. To compare the pure oxygen transport parameters in the membrane and in water, the value W_0(d-TEMPONE) in Eq. 4 was corrected by taking into account the diffusion coefficient of d-TEMPONE in water. (Corrected values are used in Fig. 2 and Table II.)

RESULTS AND DISCUSSION

Saturation–Recovery Measurement of the Oxygen Transport Parameter

The results of T_1 measurements as well as calculated values of $W(x)$ for 5-, 12-, and 16-SASL incorporated into the plasma membrane of CHO cells are presented in Table I. As expected because of oxygen-induced electron relaxation, T_1^{-1}(air) is always greater than $T_1^{-1}(N_2)$ at a given temperature using the same spin label. In addition, as shown in Table I, increasing temperature increases T_1^{-1} of the nitroxide at all three positions along the acyl chain regardless of the presence of air or nitrogen. T_1's of SASL measured in nitrogen atmosphere for the CHO plasma membrane are longer than for model membranes (Kusumi et al., 1982; Yin and

TABLE I

Spin-Lattice Relaxation Times and Oxygen Transport Parameters of SASL Incorporated into the Cell Plasma Membrane of CHO Cells

Spin Label	Temp	$1/T_1(N_2)$	$1/T_1$ (% air)	$W(x)$
	°C	μs^{-1}	μs^{-1}	μs^{-1}
			(50% air)*	
5-SASL	10	0.13 ± 0.01 (3)‡	0.23 ± 0.01 (3)	0.20 ± 0.03
	20	0.19 ± 0.02 (4)	0.43 ± 0.05 (4)	0.48 ± 0.11
	37	0.20 ± 0.01 (4)	0.55 ± 0.09 (3)	0.70 ± 0.19
			(25% air)	
12-SASL	10	0.14 ± 0.02 (3)	0.21 ± 0.01 (3)	0.28 ± 0.08
	20	0.15 ± 0.02 (3)	0.31 ± 0.03 (3)	0.64 ± 0.15
	37	0.19 ± 0.01 (4)	0.37 ± 0.04 (5)	0.72 ± 0.17
			(25% air)	
16-SASL	10	0.20 ± 0.01 (3)	0.29 ± 0.02 (4)	0.36 ± 0.08
	20	0.32 ± 0.02 (3)	0.51 ± 0.02 (3)	0.76 ± 0.10
	37	0.36 ± 0.05 (4)	0.63 ± 0.11	1.08 ± 0.48

*T_1 data were obtained for samples equilibrated with 50% air (in the case of 5-SASL) and 25% air (in the case of 12- and 16-SASL).

‡The standard deviation is calculated for the number of independent measurements given in parenthesis.

Hyde, 1987; Subczynski et al., 1989, 1991*a*). This suggests slower motion of alkyl chains in plasma membranes compared with fluid-phase model membranes. Similar results have been reported based on linewidth ESR measurements (Lai et al., 1980*b*). Addition of KCN did not affect T_1 values inasmuch as the T_1's (N_2) measured in the presence of KCN were similar to those in its absence.

Values of the oxygen transport parameter, $W(x)$, are obtained by subtracting the data in nitrogen atmosphere from the data in the presence of oxygen (see Eq. 1). An extrapolation was made to 100% air on the basis of the linear dependence of T_1^{-1} on oxygen concentration in the equilibrating gas (Kusumi et al., 1982; Yin and Hyde, 1987). The results in Table I indicate two important trends: (*a*) the value of the oxygen transport parameter in the membrane, $W(x)$, increases with temperature, and (*b*) at a given temperature, the value of $W(x)$ varies with the position of the nitroxide

along the acyl chain, being smallest at the membrane surface and greatest in the membrane center. Because nitroxide groups of SASL are located at different depths in the membrane,[3] the profile of $W(x)$ across the membrane can be plotted as in Fig. 1.

The oxygen transport parameter in the aqueous phase obtained with d-TEMPONE is also shown in Fig. 1 for comparison. The changes in $W(x)$ are due to the dependence of both the solubility and diffusion coefficient of oxygen on temperature and location in the membrane. Similar profiles of the oxygen diffusion–concentration product were obtained for fluid-phase model membranes using saturation–recovery measurements (Kusumi et al., 1982; Subczynski et al., 1989, 1991*a*) and the ESR line-broadening method (Windrem and Plachy, 1980; Subczynski, Markowska, and Sielewiesiuk, 1991*b*). A significant difference between results in the plasma membrane and those in model membranes is that all values of $W(x)$ for plasma membranes (even at 37°C) are lower than for water, while in phosphatidylcholine model membranes at physiological temperatures, $W(x)$ is greater than for water for all locations in the bilayer. It is noted that addition of a large amount of cholesterol to the model membrane (30–50 mol%) significantly decreases $W(x)$ in and near the polar head-group region (5-SASL position), but in the membrane center (16-SASL position) has little effect (dimyristoylphosphatidylcholine [DMPC]) or may even increase the values of $W(x)$ (dioleoylphosphatidylcholine [DOPC], egg yolk phosphatidylcholine [EYPC]).

Diffusion of small molecules in membranes has been related to kink formation in phospholipid alkyl chains (Träuble, 1971; Pace and Chan, 1982; Subczynski et al., 1991*a*). Decreased motion arises from a decreased number of kinks and results in lower solubility and diffusivity of oxygen. These models are consistent with decreased oxygen transport in plasma membranes compared with model membranes.

Our results also show that oxygen diffuses much more freely in the membrane center. It therefore can be inferred that all chemical reactions that are dependent on the collision frequency with oxygen (lipid peroxidation, formation of active forms of oxygen) will proceed more readily in the membrane center than in the hydrocarbon region close to the membrane surface (see Subczynski et al., 1991*b*). Further, our data support the promising hypothesis of Skulachev (1990) that extended membra-

[3] In our previous papers (Merkle, Subczynski, and Kusumi, 1987; Yin, Feix, and Hyde, 1990), we reported the existence of vertical fluctuations of nitroxide moieties of SASL toward the polar surfaces of the lipid bilayers. Measurements were made of bimolecular collision rates between nitroxide moieties at different locations on the alkyl chain. Information on the time-averaged depth, however, is not available. Vertical fluctuations are the result of alkyl chain bending rather than bobbing-like movement of the whole molecule; similar results were obtained for phosphatidylcholine spin labels (Yin, J.-J., J. B. Feix, and J. S. Hyde, unpublished data). Neutron diffraction measurement in deuterated phosphatidylcholine model membranes (Zaccai, Buldt, Seelig, and Seelig, 1979) show that average positions of the carbon atoms in the alkyl chain can be determined with an accuracy of ±1.5 Å; however, it is also reported that the width of label distribution is found to increase at the end of the chain. These measurements indicate that for most of the time carbon atoms (in our case, nitroxide moieties) stay at the positions determined by Zaccai et al. (1979). Our calculations (Subczynski et al., 1989, 1991*a*) assume that the nitroxide moiety of SASL is located at the mean depth of the 1- and 2-chains of the phosphatidylcholine membrane.

nous systems may in principle be applied as routes for intracellular oxygen transport. Oxygen transport across the cytosol seems to be less effective.

Oxygen Permeability across the CHO Plasma Membrane

$W(x)^{-1}$, which is a measure of resistance to oxygen permeation, is plotted as a function of distance from the center of the membrane in Fig. 2 *A*. Because of lack of other data, we assume that the thickness of the lipid part of the CHO plasma membrane and the locations of SASL nitroxide groups are the same as in the EYPC bilayer. For more detail, see the explanation in Table II and the method of evaluation of the thickness and nitroxide position in Subczynski et al. (1989, 1991*a*).

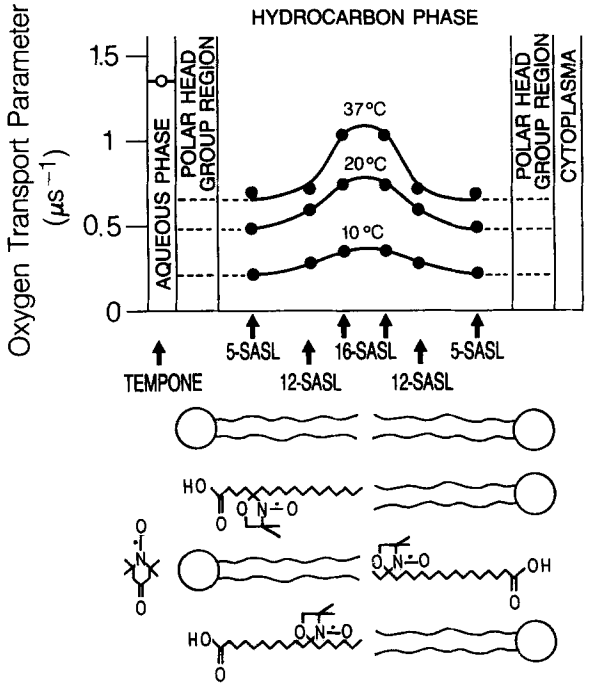

FIGURE 1. Profiles of the oxygen transport parameter across the CHO plasma membrane as a function of temperature (●). Approximate locations of nitroxide moieties of spin labels are indicated by arrows. The oxygen transport parameter in the aqueous phase is also indicated (○). It does not change significantly with temperature (1.23 μs^{-1} at 10°C and 1.35 μs^{-1} at 37°C) because the temperature dependencies of oxygen diffusion and concentration are opposite.

It is seen in Fig. 2 *A* that a moderate permeability barrier is located near the polar head-group region.

The permeability coefficient of oxygen across the CHO plasma membrane was evaluated using Eq. 3 with the integration performed based on figures such as Fig. 2 *A*. We evaluated contributions to the integral in the polar head-group region by assuming first that $W(x)$ throughout the region is the same as W(5-SASL), resulting in an upper limit value. It was then assumed that $W(x)$ changes linearly from the value at the 5-SASL position to the value for the aqueous phase, resulting in a lower limit value. The value of P_M was taken to be the mean of these two values. Support for the procedure comes from the fact that for model membranes, W(tempocholine dipalm-

itoylphosphatidic acid ester), which reports the oxygen transport parameter for the polar head-group region, lies between W(5-SASL) and W(water) (Subczynski et al., 1989, 1991*a*).

The manner of integration of the oxygen permeability coefficient across a water layer of the same thickness as a membrane is shown in Fig. 2 *B*. The ratio P_M/P_W is the ratio of these two integrals. As previously noted, by using the ratio of P_M/P_W, the effect of uncertainty of A in Eqs. 2, 3, and 4 can be reduced. The final value of P_M was obtained by multiplying P_M/P_W by the permeability value of oxygen through the

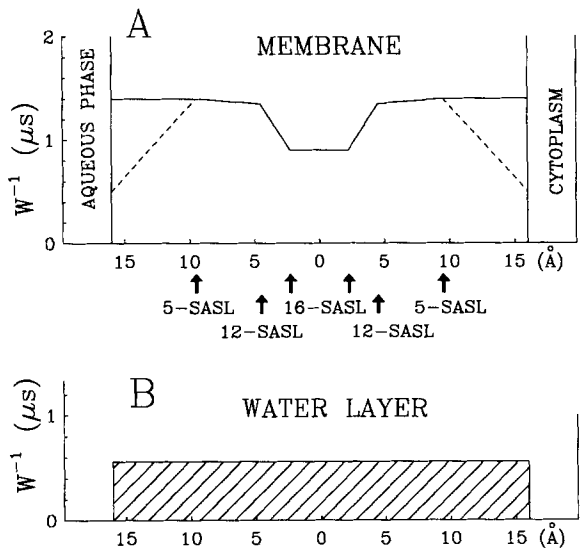

FIGURE 2. (*A*) $W(x)^{-1}$ at 37°C is plotted as a function of the distance from the center of the membrane to show the oxygen permeability barriers and the method of integration based on Eq. 3 (i.e., measuring the area under the solid and broken curves). Solid and broken lines show the maximal and minimal evaluations. The thickness of the membrane and positions of the nitroxide moieties are assumed to be the same as for EYPC bilayer (see Subczynski et al., 1989, 1991*a*). (*B*) W_0(water)$^{-1}$ at 37°C plotted for a water layer of the same thickness as the membrane in order to illustrate the method of integration following Eq. 4 (measuring the area under the solid curve). Corrected values of W_0(d-TEMPONE) were obtained by multiplying the oxygen transport parameter W(d-TEMPONE) from T_1 measurements by the factor $D_W/[D_W + D_{SL}$ (water)]. Values for the diffusion coefficient of TEMPONE in water (D_{SL}(water) = 0.9×10^{-5}, 0.6×10^{-5}, and 0.45×10^{-5} cm^2/s at 37, 20, and 10°C, respectively) were obtained from ESR line broadening data presented by Molin, Salikhov, and Zamaraev (1980). The value of 0.72×10^{-5} cm^2/s for translational diffusion of di-*t*-butyl nitroxide in water at 26°C was obtained by Ahn (1976) using a capillary diffusion method. The ratio of P_M/P_W is simply the ratio of the areas shown in the figure.

water layer as calculated from measurement of bulk diffusion constants (St. Denis and Fell, 1971). Data are in Table II. The oxygen permeability coefficient for the CHO plasma membrane is found to be smaller by a factor of 2 than that for a water layer of the same thickness as the membrane at 37°C and by a factor of 5 at 10°C. At 37°C, P_M of the CHO plasma membrane is comparable to the value of P_M of DMPC model membranes containing 50 mol% of cholesterol and is two times smaller than P_M of EYPC containing 50 mol% of cholesterol. It is, however, significantly larger than P_M for DMPC in the gel phase.

We have searched the literature for measurements of permeability coefficients that can be compared with our measurements. Gutknecht, Bisson, and Tosteson (1977) reported CO_2 permeability across an EYPC/cholesterol (1:1) bilayer of 0.35 cm/s, which is ~100 times lower than that for oxygen (Subczynski et al., 1991*a*). We are unable to explain the low value obtained in their experiment. In another paper (Princen, Overbeck, and Mason, 1967) permeabilities were obtained for eight gases across a monolayer of hexadecyltrimethylammonium using a gas bubble resting at the gas/liquid interface. Values for A, O_2, N_2, CO_2, N_2O, and Ne are very close, and lie in the permeability range from 13.6 to 39.5 cm/s. Permeabilities for He (88.5 cm/s) and H_2 (62.0 cm/s) are significantly higher, but these gases have a much higher diffusion in many solvents. Because P_M is smaller than P_W, it follows that the

TABLE II

Oxygen Permeability Coefficients for CHO Plasma Membranes

Temperature	D_w^*	$P_M/P_W^‡$	$P_W^§$	$P_M^‖$
°C	10^{-5} cm²/s		cm/s	cm/s
10	1.5	0.15	46.7	7.2
20	2.0	0.34	62.3	21.1
37	3.0	0.45	93.5	42.0

The thickness of the EYPC membrane (δ_M) was reported by Levine and Wilkins (1971) and Lis, McAlister, Fuller, and Rand (1982). The thickness of the hydrocarbon layer (δ_H) and that of the polar head group region (including the glycerol ester groups, δ_p), as well as positions of the nitroxide group of spin labels were calculated by the procedure described in our earlier papers (Subczynski et al., 1989, 1991*a*). The values are as follows: δ_M = 32.1 Å; δ_H = 24.5 Å, and δ_p = 3.8 Å. The nitroxide group of 5-, 12-, and 16-SASL are located at distances of 9.45, 4.55, and 1.75 Å, respectively, from the membrane center.

*The bulk diffusion coefficient of molecular oxygen in water (St. Denis and Fell, 1971).

‡This ratio was determined from P_M and P_W, both of which were determined in the pulse ESR spin-label experiment.

§Oxygen permeability coefficient across the water layer that has the same thickness as the membrane (calculated from the membrane thickness and D_W according to Eq. 5).

‖P_M was determined by multiplying P_W determined from the bulk diffusion coefficient and the P_M/P_W ratio determined by the present spin-label method. In this way, uncertainties of p and r_0 can be avoided (see Eq. 2).

membrane will be a barrier for oxygen permeation. Our data indicate that for CHO cells at physiological conditions, oxygen concentration differences across the cell plasma membrane will be about two times greater than those across a water layer of the same thickness.

Our results (Table II) show a greater temperature variation for P_M than for P_W, which is consistent with the results of other investigators. If it is assumed that $D(x)$ and $C(x)$ Eq. 2 are constants, Eq. 3 becomes $P_M = D_M K_M/\delta_M$. We also have Eq. 5: $P_W = D_W/\delta_M$. Lieb and Stein (1986) report that D_M exhibits a greater temperature dependence than D_W, both values increasing with temperature. In addition, K_M for nonelectrolytes and gases also increases with temperature (Power and Stegall, 1970; Katz and Diamond, 1974; Dix, Kivelson, and Diamond, 1978; Subczynski and Hyde, 1983; Smotkin, Moy, and Plachy, 1991).

GENERAL DISCUSSION AND CONCLUSIONS

Boag (1969) gives expressions for the profile of oxygen concentration outside and inside a spherical cell assuming uniform consumption of oxygen within the cell.

$$C(r) = C_\infty - \frac{V}{4\pi RD}\left(\frac{R}{r}\right) \quad r > R \tag{6}$$

$$C(r) = C_\infty - \frac{3V}{8\pi RD}\left(1 - \frac{r^2}{3R^2}\right) \quad r < R \tag{7}$$

where R is the radius of the cell, V is the oxygen consumption rate per cell, and D is the diffusion coefficient of oxygen (assuming that D is the same both inside and outside of the cell). Boag (1969) assumed that the drop of oxygen concentration across the cell plasma membrane is negligible. Knowledge of the membrane permeability, P_M, allows us to add the missing term to Eq. 7.

$$C(r) = C_\infty - \Delta C_M - \frac{3V}{8\pi RD}\left(1 - \frac{r^2}{3R^2}\right) r < R \tag{8}$$

where

$$\Delta C_M = \frac{V}{4\pi R^2 P_M} \tag{9}$$

or equivalently,

$$\Delta C_M = \frac{V}{4\pi RD}\left(\frac{\delta_M}{R}\frac{P_W}{P_M}\right) \tag{10}$$

Under conditions where enzymatic control limits respiration, ΔC_M can be calculated from published data: $V = 6 \times 10^{-17}$ mol of O_2 s^{-1} per cell (Lai et al., 1982), $R = 8.2$ μm (Lai et al., 1980*b*), $D = 3 \times 10^{-5}$ cm^2 s^{-1} (St. Denis and Fell, 1971), and $\delta_M = 32$ Å (see footnote to Table II). We obtain $\Delta C_M = 0.3$ nM. The profile of oxygen concentration arising from oxygen consumption of a spherical cell is shown schematically in Fig. 3.

Gradients inside and outside the cell can be calculated by taking the derivatives of Eqs. 6 and 8 with respect to r.

$$\frac{\partial C(r)}{\partial r} = \frac{V}{4\pi Dr^2} \quad r > R \tag{11}$$

$$\frac{\partial C(r)}{\partial r} = \frac{Vr}{4\pi DR^3} \quad r < R \tag{12}$$

These can be compared with the gradient in the membrane

$$\frac{\Delta C_M}{\delta_M} = \frac{V}{4\pi DR^2}\frac{P_W}{P_M} \tag{13}$$

It is apparent from Eqs. 11 and 12 that the maximum possible gradients in the medium, both inside and outside the cell, occur at the cell surface, where both

expressions yield

$$\left(\frac{\partial C(r)}{\partial r}\right)_{r=R} = \frac{V}{4\pi DR^2} \tag{14}$$

a value that is about half of that given by Eq. 13.

The "barrier" presented by the external medium is the integral of the gradient, Eq. 11, from $r = R$ to ∞, yielding, trivially, the concentration difference from Eq. 6, $\Delta C_{\text{external}}$.

$$\Delta C_{\text{ext}} = \frac{V}{4\pi RD} \tag{15}$$

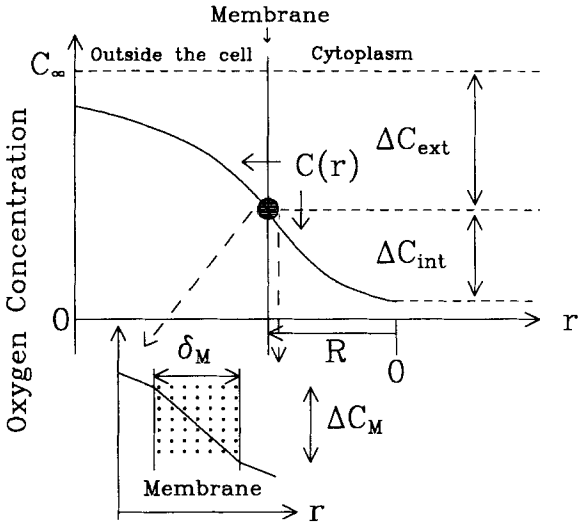

FIGURE 3. Profile of oxygen concentration and concentration differences formed by oxygen consumption by a spherical cell (radius R). The oxygen consumption rate within the cell is assumed to be uniform. Three regions are considered separately (Eqs. 6–10): (*1*) From infinity to the cell membrane, $\Delta C_{\text{ext}} = V/4\pi RD$. (*2*) From the cell membrane to the center of the cell, $\Delta C_{\text{int}} = V/8\pi RD$. (*3*) The oxygen concentration difference across the cell plasma membrane, $\Delta C_M = (V/4\pi RD)(\delta_M P_W/RP_M)$. Oxygen concentration differences calculated for a respirating CHO cell at 37°C are: ΔC_{ext} = 200 nM, ΔC_{int} = 100 nM, and ΔC_M = 0.3 nM.

(We apologize to the reader for tediously differentiating and then integrating, but we strive for precision in the use of the words "barrier" and "gradient.") This can be compared with the barrier presented by the membrane ΔC_M in Eq. 10. One sees immediately that the oxygen consumption rate V can play no role in determining whether or not the membrane is a barrier to respiration. The barrier presented by the membrane can only be significant when

$$\frac{\delta_M}{R}\frac{P_W}{P_M} \approx 1 \tag{16}$$

Recall that P_W is the permeability of a layer of water of the same thickness as the membrane. Since the ratio $P_W/P_M \approx 2$, this study leads to the conclusion that the

membrane of the CHO cell can never be a barrier that significantly affects oxygen consumption even at rates of oxygen tension near the apparent Michaelis-Menten constant. And, furthermore, for any systems with membranes of the same permeability as that of CHO cells, the membrane can be a barrier only if R is very small, becoming comparable indeed to the membrane thickness itself.

The extension of these conclusions to other cell systems and to organelles must depend on membrane constituents and their effect on oxygen transport. Cholesterol at high concentration decreases the P_M of model membranes (Subczynski et al., 1989, 1991*a*). It is accepted that cholesterol is especially abundant in the plasma membrane of mammalian cells; however, we have no exact data for CHO cells. Available data show only that the amount of cholesterol in the particulate fraction of CHO cells is 1.7 $\mu g/10^6$ cells (Cress, Culver, Moon, and Gerner, 1982). The molar ratio of cholesterol/phospholipid lies between 0.4 and 0.5 (Rintoul, Sklar, and Simoni, 1978; Cress and Gerner, 1980; Cress et al., 1982). The amount of cholesterol per CHO cell is lower than for other lines (Cress et al., 1982). However, the ratio of cholesterol/phospholipid is rather typical. It would appear from this survey of the literature taken together with the results presented here that variations of cholesterol content among various membranous systems are not likely to be the determining factor in affecting respiration.

Data do exist indicating that protein content in the membrane can affect the oxygen permeability coefficient. See, for example, Kawasaki, Yin, Subczynski, Hyde, Ohnishi, and Kusumi, 1988; Altenbach, Marti, Khorana, and Hubbell, 1990; Ashikawa, Yin, Subczynski, Hyde, and Kusumi, 1990. These studies, however, introduce another level of complication: they demonstrate variations of oxygen transport between bulk lipid and boundary layers of proteins, between protein clusters and bulk lipids, between lipid domains, and within the integral membrane protein itself.

The protein content in mammalian cell plasma membranes is rather low. Typical protein to lipid ratios (wt/wt) lie between 0.4 and 1.5, compared with a ratio of 3.0 in protein-rich membranes (halobacterium purple membrane or mitochondrial inner membrane) and a ratio of 0.18 in protein-poor membrane (myelin) (Guidotti, 1972). On the basis of data available in the literature (Juliano and Behar-Bannelier, 1975; Cress et al., 1982; Nettleton et al., 1988), we estimate the protein to lipid ratio (wt/wt) in CHO cell plasma membranes to be less than or equal to 1.0. Although it is established that substantial local variations in oxygen transport exist, it does not appear that the average permeability of the mammalian membrane can be sufficiently altered by variations in protein content that the membrane itself can become a diffusion-limitation barrier that affects respiration.

As mentioned in the Introduction, it is possible that SASL is redistributed among all cell membranes. In this event, we measure the average oxygen transport parameters through the lipid bilayer portion of all membranes (the total plasma membrane lipid of the CHO cell consists of only 7% of the cell's total lipid content [Nettleton et al., 1988]). If SASL is distributed between all cell membranes, it could only decrease the evaluation of P_M because of the contribution of membranes rich in integral proteins such as the mitochondria and endoplasmic reticulum. If this is indeed the case, the oxygen permeability of the CHO plasma membrane reported here is a lower limit. It might be even closer to that of the bulk medium.

Finally, we compare oxygen permeability across a lipid bilayer with the permeabilities of other small nonelectrolytes. We use data collected by Walter and Gutknecht (1986) for the diffusion across an EYPC bilayer of nonelectrolytes having molecular weights smaller than 300. These authors studied Overton's rule. They plotted the permeability of various nonelectrolyte solutes across EYPC versus the partition coefficient of the solute between organic solvent and water according to the equation

$$\log P_M = s \log K + b \tag{17}$$

This relation can also be written in the form

$$P_M = cK^S \tag{18}$$

where

$$b = \log c \tag{19}$$

A total of 24 solute P_M, K pairs were studied in four solvents: hexadecane, olive oil, octanol, and ether. They found higher correlation coefficients in hexadecane and olive oil if the seven solutes of mol wt < 50 are omitted.

They did not plot the data for the seven small molecules according to Eq. 17. We have done so, and have added our own data for the permeability of oxygen through EYPC (Subczynski et al., 1991*a*) together with values of oxygen partition coefficients from the literature (Macey, 1948; Battino, Evans, and Danforth, 1968) (see Fig. 4). A very good fit to Eq. 17 is obtained. Parameters s and b together with the correlation

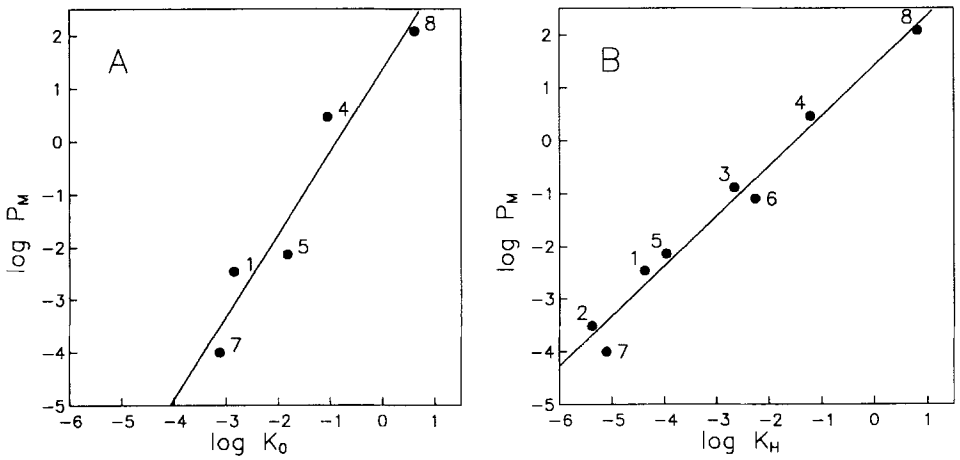

FIGURE 4. The permeability coefficient (P_M) across an EYPC bilayer is plotted against the partition coefficients at 25°C between olive oil and water (*A*) and between hexadecane and water (*B*). Solutes are numbered as follows: *1*, water; *2*, hydrofluoric acid; *3*, ammonia; *4*, hydrochloric acid; *5*, formic acid; *6*, methylamine; *7*, formamide; *8*, oxygen. Data for solutes 1–7 are taken from Walter and Gutknecht (1986) and for solute *8* from Subczynski et al. (1991*a*) (P_M); Battino et al. (1968) (K_0); and Macey (1948) (K_H).

coefficient r are given in Table III. The table also contains the parameters given by Walter and Gutknecht (1986) using solutes of 50 < mol wt < 300.

The main conclusion from Fig. 4 and Table III is that the behavior of oxygen is fully compatible with that of other nonelectrolyte solutes of mol wt < 50 over a range of 4×10^5 in permeabilities and 10^6 in partition coefficients. A further conclusion, also emphasized by Walter and Gutknecht (1986), is that a significant change in membrane transport mechanisms for small nonelectrolytes occurs at mol wt = 50.

We have not found a precise and widely accepted definition of Overton's rule, but we are of the opinion from our reading of the literature that this rule requires a linear dependence between membrane permeability and partition coefficient. For solutions of mol wt < 50, Overton's rule is not followed using olive oil. For hexadecane, the rule is approximately satisfied for all molecular weight solutes of mol wt < 300, but correlation coefficients are improved if solutes are grouped into those with mol wt < 50 and mol wt > 50, with slightly adjusted parameters.

It is concluded that: (*1*) The oxygen permeability coefficient can be evaluated for

TABLE III

Least-Squares Regression Analyses of EYPC Membrane Permeabilities (P_M) and Partition Coefficients (K) into Two Organic Solvents, Plotted According to the Relation, log P_M = s log K + b

Model solvent	Number of solutes*	Correlation coefficient (r)	Slope (s)	Intercept (b)
Hexadecane	16 (50 < mW < 300)	0.995	1.06	1.10
	8 (mW < 50)	0.987	0.95	1.42
	24‡ (mW < 300)	0.977	0.977	1.12
Olive oil	11 (50 < mW < 300)	0.990	1.11	−0.67
	5 (mW < 50)	0.964	1.56	1.36

*For details see text and Fig. 4 legend.

‡Analyses include all P_M and K pairs including oxygen.

biological membranes based on the profiles of the oxygen transport parameter. (*2*) A rule can be formulated to predict membrane permeability coefficients for small nonelectrolyte solutes (mol wt < 50), including oxygen, from partition coefficients into hexadecane and olive oil, although the linear dependence between membrane permeability and partition coefficient is observed only for hexadecane as a model solvent. (*3*) The oxygen concentration difference created across the cell plasma membrane during oxygen consumption by the cell is of the order of magnitude of nanomolar. (*4*) The cell plasma membrane is not a barrier for oxygen transport to the cell and cannot influence or regulate the oxygen consumption rate.

The authors wish to thank Dr. Ching-San Lai for many helpful discussions and critical reading of the manuscript.

This work was supported by grants GM-22923, GM-27665, and RR-01008 from the National Institutes of Health.

Original version received 21 October 1991 and accepted version received 27 March 1992.

REFERENCES

Ahn, M.-K. 1976. Diffusion coefficients of paramagnetic species in solution. *Journal of Magnetic Resonance.* 22:289–293.

Altenbach, C., T. Marti, H. G. Khorana, and W. L. Hubbell. 1990. Transmembrane protein structure: spin labeling of bacteriorhodopsin mutants. *Science.* 248:1088–1092.

Ashikawa, I., J.-J. Yin, W. K. Subczynski, J. S. Hyde, and A. Kusumi. 1990. Effect of an integral membrane protein on oxygen transport in reconstituted membranes of bacteriorhodopsin. *Proceedings of the 10th International Biophysics Congress.* 258. (Abstr.)

Bales, B. L., and V. Leon. 1978. Magnetic resonance studies of eucaryotic cells. III. Spin labeled fatty acids in the plasma membrane. *Biochimica et Biophysica Acta.* 509:90–99.

Bales, B. L., E. S. Lesin, and S. B. Oppenheimer. 1977. On cell membrane lipid fluidity and plant lectin agglutinability: a spin label study of mouse ascites tumor cells. *Biochimica et Biophysica Acta.* 465:400–407.

Battino, R., F. D. Evans, and W. F. Danforth. 1968. Solubilities of seven gases in olive oil with reference to theories of transport through the cell membrane. *Journal of the American Oil Chemists' Society.* 45:830–833.

Boag, J. W. 1969. Oxygen diffusion and oxygen depletion problems in radiobiology. *Current Topics in Radiation Research.* 5:141–195.

Coin, D. T., and J. S. Olson. 1979. The rate of oxygen uptake by human red blood cells. *Journal of Biological Chemistry.* 254:1178–1190.

Cress, A. E., P. S. Culver, T. E. Moon, and E. W. Gerner. 1982. Correlation between amounts of cellular membrane components and sensitivity to hyperthermia in a variety of mammalian cell lines in culture. *Cancer Research.* 42:1716–1721.

Cress, A. E., and E. W. Gerner. 1980. Cholesterol levels inversely reflect the thermal sensitivity of mammalian cells in culture. *Nature.* 283:677–679.

Diamond, J. M., and Y. Katz. 1974. Interpretation of nonelectrolyte partition coefficients between dimyristoyl lecithin and water. *Journal of Membrane Biology.* 17:121–154.

Dix, J. A., D. Kivelson, and J. M. Diamond. 1978. Molecular motion of small nonelectrolyte molecules in lecithin bilayers. *Journal of Membrane Biology.* 40:315–342.

Dodd, N. J. E., S. L. Schor, and G. Rushton. 1982. The effects of a collagenous extracellular matrix of fibroblast membrane organization: an ESR spin label study. *Experimental Cell Research.* 141:421–431.

Fischkoff, S., and J. M. Vanderkooi. 1975. Oxygen diffusion in biological and artificial membranes determined by the fluorochrome pyrene. *Journal of General Physiology.* 65:663–676.

Froncisz, W., and J. S. Hyde. 1982. The loop-gap resonator: a new microwave lumped circuit ESR sample structure. *Journal of Magnetic Resonance.* 47:515–521.

Froncisz, W., C.-S. Lai, and J. S. Hyde. 1985. Spin-label oximetry: kinetic study of cell respiration using a rapid passage T_1 sensitive electron spin resonance display. *Proceedings of the National Academy of Sciences, USA.* 82:411–415.

Gaffney, B. J. 1975. Fatty acid chain flexibility in the membranes of normal and transformed fibroblasts. *Proceedings of the National Academy of Sciences, USA.* 72:664–668.

Glockner, J. F., H. M. Swartz, and M. A. Pals. 1989. Oxygen gradients in CHO cells: measurement and characterization by electron-spin resonance. *Journal of Cellular Physiology.* 140:505–511.

Guidotti, G. 1972. Membrane proteins. *Annual Review of Biochemistry.* 41:731–752.

Gutknecht, J., M. A. Bisson, and F. C. Tosteson. 1977. Diffusion of carbon dioxide through lipid bilayer membranes. Effects of carbonic anhydrase, bicarbonate and unstirred layers. *Journal of General Physiology.* 69:779–794.

Hill, R. P., and M. G. Pallavicini. 1983. Hypoxia and the radiation response of tumors. *Advances in Experimental Medicine and Biology.* 159:17–35.

Huisjen, M., and J. S. Hyde. 1974. A pulsed EPR spectrometer. *Review of Scientific Instruments.* 45:669–675.

Huxley, V. H., and M. J. Kutchai. 1981. The effect of the red cell membrane and a diffusion boundary layer on the rate of oxygen uptake by human erythrocytes. *Journal of Physiology.* 316:75–83.

Huxley, V. H., and M. J. Kutchai. 1983. Effects of diffusion boundary layers on the initial uptake of oxygen by red blood cells: theory *vs.* experiments. *Microvascular Research.* 26:89–107.

Hyde, J. S., and W. K. Subczynski. 1984. Simulation of ESR spectra of the oxygen-sensitive spin-label probe CTPO. *Journal of Magnetic Resonance.* 56:125–130.

Hyde, J. S., and W. K. Subczynski. 1989. Spin-label oximetry. *In* Biological Magnetic Resonance. Vol. 8. Spin Labeling: Theory and Applications. L. J. Berliner and J. Reubens, editors. Plenum Publishing Corp., New York. 399–425.

Jones, D. P. 1984. Effect of mitochondrial clustering on O_2 supply in hepatocytes. *American Journal of Physiology.* 47(*Cell Physiology* 16)C:83–89.

Jones, D. P., and F. G. Kennedy. 1982. Intracellular oxygen gradients in cardiac myocytes: lack of a role for myoglobin in facilitation of intracellular oxygen diffusion. *Biochemical and Biophysical Research Communications.* 105:419–424.

Juliano, R. L., and M. Behar-Bannelier. 1975. An evaluation of techniques for labeling the surface proteins of cultured mammalian cells. *Biochimica et Biophysica Acta.* 375:249–267.

Kalyanaraman, B., J. B. Feix, F. Sieber, J. P. Thomas, and A. W. Girotti. 1987. Photodynamic action of merocyanine 540 on artificial and natural cell membranes: involvement of singlet molecular oxygen. *Proceedings of the National Academy of Sciences, USA.* 84:2999–3003.

Kaplan, J., P. G. Canonico, and W. J. Caspary. 1973. Electron spin resonance studies of spin-labeled mammalian cells by detection of surface-membrane signals. *Proceedings of the National Academy of Sciences, USA.* 70:66–70.

Katz, I. R., J. B. Wittenberg, and B. A. Wittenberg. 1984. Monoamine oxidase an intracellular probe of oxygen pressure in isolated cardiac myoctes. *Journal of Biological Chemistry.* 259:7504–7509.

Katz, Y., and J. M. Diamond. 1974. Thermodynamic constants for nonelectrolyte partition between dimyristoyl lecithin and water. *Journal of Membrane Biology.* 17:101–120.

Kawasaki, K., J.-J. Yin, W. K. Subczynski, J. S. Hyde, S. Ohnishi, and A. Kusumi. 1988. Observation of lipid exchange reaction between two domains in the outer membrane of influenza virus by a pulse ESR spin labeling method. *Proceedings of the XIII International Conference on Magnetic Resonance in Biological Systems.* 13–31. (Abstr.)

Kusumi, A., W. K. Subczynski, and J. S. Hyde. 1982. Oxygen transport parameter in membranes as deduced by saturation recovery measurements of spin-lattice relaxation times of spin labels. *Proceedings of the National Academy of Sciences, USA.* 79:1854–1858.

Lai, C.-S., L. E. Hopwood, J. S. Hyde, and S. Lukiewicz. 1982. ESR studies of O_2 uptake by Chinese hamster ovary cells during the cell cycle. *Proceedings of the National Academy of Sciences, USA.* 79:1166–1170.

Lai, C.-S., L. E. Hopwood, and H. M. Swartz. 1980*a*. ESR studies on membrane fluidity of Chinese hamster ovary cells grown on microcarriers and in suspension. *Experimental Cell Research.* 130:437–442.

Lai, C.-S., L. E. Hopwood, and H. M. Swartz. 1980*b*. Electron spin resonance studies of changes in membrane fluidity of Chinese hamster ovary cells during the cell cycle. *Biochimica et Biophysica Acta.* 602:117–126.

Levine, Y. K., and M. H. F. Wilkins. 1971. Structure of oriented lipid bilayers. *Nature, New Biology.* 230:69–72.

Lieb, W. R., and W. D. Stein. 1986. Simple Diffusion across the Membrane Bilayer. *In* Transport and Diffusion across Cell Membranes. W. D. Stein, editor. Academic Press, Orlando, FL. 69–112.

Lis, L. J., M. McAlister, N. Fuller, and R. P. Rand. 1982. Interactions between neutral phospholipid bilayer membranes. *Biophysical Journal.* 37:657–666.

Macey, R. 1948. Partition coefficients of fifty compounds between olive oil and water. *Journal of Industrial Hygiene and Toxicology.* 30:140–143.

McCord, J. M. 1985. Oxygen-derived free radicals in postischemic tissue injury. *New England Journal of Medicine.* 312:159–163.

McDonald, G. C., J. M. Vanderkooi, and J. C. Oberholtzer. 1979. Oxygen diffusion in phospholipid artificial membranes studied by Fourier transform nuclear magnetic resonance. *Archives of Biochemistry and Biophysics.* 196:281–283.

Merkle, H., W. K. Subczynski, and A. Kusumi. 1987. Dynamic fluorescence quenching studies on lipid mobilities in phosphatidylcholine-cholesterol membranes. *Biochimica et Biophysica Acta.* 897:238–248.

Molin, Y. N., K. M. Salikhov, and K. I. Zamaraev. 1980. Spin Exchange. Springer-Verlag New York Inc., New York. 111–115.

Morse, P. D., II, and H. M. Swartz. 1985. Measurement of intracellular oxygen concentration using the spin label TEMPOL. *Magnetic Resonance in Medicine.* 2:114–117.

Nettleton, D. O., P. D. Morse II, J. W. Dobrucki, H. M. Swartz, and N. J. F. Dodd. 1988. Distribution of 5-doxylstearic acid in the membranes of mammalian cells. *Biochimica et Biophysica Acta.* 944:315–320.

Pace, R. J., and S. I. Chan. 1982. Molecular motions in lipid bilayers. III. Lateral and transversal diffusion in bilayers. *Journal of Chemical Physics.* 76:4241–4247.

Power, G. G., and H. Stegall. 1970. Solubility of gases in human red blood cell ghosts. *Journal of Applied Physiology.* 29:145–149.

Princen, H. M., J. T. G. Overbeck, and S. G. Mason. 1967. The permeability of soap films to gases. II. A simple mechanism of monolayer permeability. *Journal of Colloid and Interface Science.* 24:125–130.

Rintoul, D. A., L. A. Sklar, and R. D. Simoni. 1978. Membrane lipid modification of Chinese hamster ovary cells. Thermal properties of membranes phospholipids. *Journal of Biological Chemistry.* 253:7447–7452.

Skulachev, V. P. 1990. Power transmission along biological membranes. *Journal of Membrane Biology.* 114:97–112.

Smotkin, E. S., F. T. Moy, and W. Z. Plachy. 1991. Dioxygen solubility in aqueous phosphatidylcholine dispersion. *Biochimica et Biophysica Acta.* 1061:33–38.

St. Denis, C. E., and C. J. Fell. 1971. Diffusivity of oxygen in water. *Canadian Journal of Chemical Engineering.* 49:885.

Struve, W. G., R. M. Arneson, J. E. Chenevey, and C. K. Cartwright. 1977. The effect of culture conditions on the fluidity of mouse neuroblastoma membranes as estimated by spin label studies. *Experimental Cell Research.* 109:381–387.

Subczynski, W. K., and J. S. Hyde. 1981. The diffusion-concentration product of oxygen in lipid bilayers using the spin-label T_1 method. *Biochimica et Biophysica Acta.* 643:283–291.

Subczynski, W. K., and J. S. Hyde. 1983. Concentration of oxygen in lipid bilayers using a spin-label method. *Biophysical Journal.* 41:283–286.

Subczynski, W. K., and J. S. Hyde. 1984. Diffusion of oxygen in water and hydrocarbons using an electron spin resonance spin-label technique. *Biophysical Journal.* 45:743–748.

Subczynski, W. K., J. S. Hyde, and A. Kusumi. 1989. Oxygen permeability of phosphatidylcholine-cholesterol membranes. *Proceedings of the National Academy of Sciences, USA.* 86:4474–4478.

Subczynski, W. K., J. S. Hyde, and A. Kusumi. 1992*a*. Effect of alkyl chain unsaturation and cholesterol intercalation on oxygen transport in membranes: a pulse ESR spin labeling study. *Biochemistry.* 30:8578–8590.

Subczynski, W. K., and E. Markowska. 1992. Effect of carotenoids on oxygen transport within and across model membranes. *Zagadnienia Biofizyki Wspolczesnej.* In press.

Subczynski, W. K., E. Markowska, and J. Sielewiesiuk. 1991*b*. Effect of polar carotenoids on the oxygen diffusion-concentration product in lipid bilayers: an ESR spin label study. *Biochimica et Biophysica Acta.* 1068:68–72.

Swartz, H. M., and M. A. Pals. 1988. Measurement of intracellular oxygen. *In* Handbook of Free Radicals and Antioxidants in Medicine. J. Miquel, A. T. Quintanilha, and H. Weber, editors. CRC Press, Inc., Boca Raton, FL. 141–151.

Tamura, M., N. Oshino, B. Chance, and I. A. Silver. 1978. Optical measurements of intracellular oxygen concentration of rat heart *in vitro*. *Archives of Biochemistry and Biophysics.* 191:8–22.

Träuble, H. 1971. The movement of molecules across lipid membranes: a molecular theory. *Journal of Membrane Biology.* 4:193–208.

Vanderkooi, J. M., W. W. Wright, and M. Erecinska. 1990. Oxygen gradients in mitochondria examined with delayed luminescence from excited-state triple probes. *Biochemistry.* 29:5332–5338.

Walter, A., and J. Gutknecht. 1986. Permeability of small nonelectrolytes through lipid bilayer membranes. *Journal of Membrane Biology.* 90:207–217.

Windrem, D. A., and W. Z. Plachy. 1980. The diffusion-solubility of oxygen in lipid bilayers. *Biochimica et Biophysica Acta.* 600:655–665.

Wittenberg, B. A., and J. B. Wittenberg. 1985. Oxygen pressure gradients in isolated cardiac myocytes. *Journal of Biological Chemistry.* 260:6548–6554.

Wittenberg, B. A., and J. B. Wittenberg. 1989. Transport of oxygen in muscle. *Annual Review of Physiology.* 51:857–878.

Yin, J.-J., J. B. Feix, and J. S. Hyde. 1990. Mapping collision frequencies for stearic acid spin labels by saturation-recovery electron paramagnetic resonance. *Biophysical Journal.* 58:713–720.

Yin, J.-J., and J. S. Hyde. 1987. Spin-label saturation-recovery electron spin resonance measurements of oxygen transport in membranes. *Zeitschrift für Physikalische Chemie Neue Folge.* 153:57–65.

Zaccai, G., G. Buldt, A. Seelig, and J. Seelig. 1979. Neutron diffraction studies on phosphatidylcholine model membranes: chain conformation and segmental disorder. *Journal of Molecular Biology.* 134:693–706.